Transcriptome Analysis of the Effect of Diosgenin on Autoimmune Thyroiditis in A Rat Model

Chengfei Zhang
Dongfang Hospital of Beijing University of Chinese Medicine
Lingling Qin
Technology Department, Beijing University of Chinese Medicine
Boju Sun
Dongfang Hospital of Beijing University of Chinese Medicine
You Wu
Dongfang Hospital of Beijing University of Chinese Medicine
Fengying Zhong
Dongfang Hospital of Beijing University of Chinese Medicine
Lili Wu
Key Laboratory of TCM Health Cultivation of Beijing, Beijing University of Chinese Medicine
Tonghua Liu (thliu@vip.163.com)
Key Laboratory of TCM Health Cultivation of Beijing, Beijing University of Chinese Medicine

Research Article

Keywords: diosgenin, autoimmune thyroiditis, rats, transcriptome, cAMP signaling pathway.

Posted Date: December 15th, 2020

DOI: https://doi.org/10.21203/rs.3.rs-121386/v1

Version of Record: A version of this preprint was published at Scientific Reports on March 18th, 2021. See the published version at https://doi.org/10.1038/s41598-021-85822-1.

Abstract

Transcriptomics was used to analyze the protective effect of diosgenin on autoimmune thyroiditis (AIT) in rats and its possible mechanism. Forty AIT model rats were established following high iodine induction and injection of porcine thyroglobulin adjuvant into Lewis rats. AIT-model rats were treated with an oral gavage(diosgenin) for 8 weeks. The concentrations of T3, T4, FT3, FT4, TSH, TRAb, TPOAb and TgAb in rat serum were detected. The unilateral thyroid lobes of rats were detected by transcriptomes, RT-qPCR (S100A9, PKA, Creb, Epac, and Rap1 mRNA), and Immunohistochemistry (cAMP, PKA, and Creb). The results showed that the expression of serum T3, T4, FT3, FT4, TSH, TgAb, and TPOAb in the high-dose group was greater than that in the low and middle-dose groups. And compared with the AIT-model group, the relative expression of cAMP, PKA and Creb mRNA and protein increased, S100A9 mRNA decreased in the diosgenin groups. To sum up, diosgenin can improve the expression of T3, T4, FT3, FT4, and TSH in AIT model rats, and decrease the concentrations of TRAb, TgAb and TPOAb, which may be related to activation of the cAMP/PKA/Creb pathway and downregulating the expression of S100A9 gene.

Introduction

Autoimmune thyroiditis (AIT), the most common expressions of which are Hashimoto's disease and Graves' disease (GD), is an organ-specific autoimmune disease characterized by the destruction of thyroid structure and hypofunction, which is caused by lymphocyte infiltration following the invasion of autoantibodies, mainly thyroid peroxidase (TPOAb) and thyroglobulin (TgAb) into the thyroid tissue [1]. High titers of TgAb exist in most patients with AIT (40%–70%), and TPOAbs are present in most patients with AIT (>80%) [2]. TSH receptor antidoby (TRAb) stimulates the TSH receptor on thyroid cells in patients[3], leading to increased thyroid hormone production and release, which is more common in Graves' disease. Generally, the diagnosis can be confirmed by B-ultrasound and antibodies in the clinic. The prevalence of AIT is increasing year by year, and the incidence in women is much higher than that in men[4].

Diosgenin is a well-known steroidal sapogenin, which can be used to treat various diseases[5]. This substance is widely found in several plants, such as species of Paris, *Costus speciosus*, *Trigonella foenum*, Aletris and Trillum, species of Dioscorea, and *Smilax menispermoidea*[6]. In *in vitro* thyroid experiments, diosgenin intervention can lead to G0/G1 arrest of thyroid cells and inhibition of insulin-like growth factors -1(IGF -1) -induced proliferation of primary human thyroid cells [7]. The ability of diosgenin to inhibit excessive proliferation of thyroid cells to a certain extent may underlie its potential therapeutic effect on Graves' disease. In further *in vivo* experiments of diosgenin, it was found to reduced goiters in a Graves' disease murine model by inhibiting the proliferation of thyroid cells. The mechanism is related to inhibiting the expression of IGF-1, nuclear factor kappa-B (NF-κB), Cyclin D1, and Proliferating Cell Nuclear Antigen (PCNA)[8] .

However, there has been little research regarding the effect of diosgenin on AIT, and the mechanism of the therapeutic effect is still unclear. To fully understand the therapeutic effect and molecular mechanism of diosgenin, we detected the concentration of serum triiodothyronine (T3), thyroxine (T4), free triiodothyronine(FT3), free thyroxine (FT4), thyroid-stimulating hormone(TSH), TSH receptor antidoby (TRAb), thyroglobulin antibodies (TgAb) and thyroid peroxidase antibody (TPOAb) and observed pathological changes in thyroid tissue *in vivo*. Transcriptome sequencing was used to study the effect of diosgenin on whole gene expression in the thyroid tissue of AIT rats. The purpose of this study was to observe the protective effect of diosgenin on an AIT model in rats and explore its possible mechanism.

Results

1 Serum expression of thyroid function

Compared with the normal group, serum levels of T3(from 0.91 to 1.62 ng/ml), T4(from 46.75 to 86.41 ng/ml), FT3(from 1.85 to 3.57 pg/ml), FT4(from 3.12 to 5.61 pg/ml) in the AIT-model group increased significantly ($P < 0.01$), while TSH decreased from 4.37 to 2.16 uIU/ml ($P < 0.01$). Compared with the AIT-model group, in the diosgenin-H group the concentrations of T3 decreased from 1.62 to 1.33 ng/ml with $P<0.05$, T4 decreased from 86.41 to 65.37 ng/ml with $P<0.01$, FT3 decreased from 3.57 to 2.66 pg/ml with $P<0.01$, and FT4 decreased from 5.61 to 4.20 pg/ml with $P<0.05$. And TSH increased from 2.16 to 3.34 uIU/ml in the diosgenin-H group with $P<0.01$. (Table 1)

2 Thyroid serum antibody expression

Compared with the normal group, concentrations of TgAb (from 24.30 to147.85 IU/ml), TPOAb(from10.56 to168.15 IU/ml) and TRAb(from 0.94 to 24.85 IU/L) in the AIT-model group increased significantly ($P < 0.01$). Compared with the AIT-model group, in the diosgenin-H group the concentrations of TgAb decreased from 147.85 to 80.94 IU/ml ($P<0.01$) and TPOAb decreased from 168.15 to 99.94 IU/ml ($P<0.01$), and in the diosgenin-M group the concentrations of TRAb decreased from 24.85 to 21.44 IU/ml ($P<0.05$) (Table 2).

3 Pathological changes in thyroid tissue

A large number of intact thyroid follicles were found in the normal group. These had moderate size, were uniformly filled with red colloid, and contained intact follicular epithelial cells. In the AIT-model group, the stroma of the thyroid follicles showed diffuse lymphocyte infiltration, with a large number of follicular cavities being destroyed or reduced; the colloid within the cavities was unevenly distributed or reduced, and the follicular wall was thin or damaged. Compared with the AIT-model group, lymphocyte infiltration into the thyroid follicular stroma in the three treatment groups was significantly decreased, follicular epithelial cells were more complete, colloid content was slightly decreased, and follicular structure was complete. The high-dose group had a slightly healthier profile than the low- and middle-dose groups. See Figure 1.

4 Transcriptome

4.1 RNA extraction and library preparation

The total RNA quality of all samples met the experimental requirements (RIN ≥ 7 and 28S/18S ≥ 0.7). The quality inspection results are shown in the supplementary materials.

4.2 Analysis of DEGs:Screening and expression level analysis of differential genes

DESeq software was used to analyze the number of DEGs: in the diosgenin group this was 79, with 54 up-regulated and 25 down-regulated compared with the AIT-model group. The overall distribution of DEGs was investigated by drawing a volcano map, as shown in Figure 2. Further, we carried out unsupervised hierarchical clustering on DEGs. Generally speaking, the same type of samples appear in the same clusters, and genes clustered together may have similar biological functions. See Figure 3 for cluster analysis results of differences among groups.

4.3 GO enrichment analysis of differential genes

In the results of GO analysis, there were no differentially expressed genes in autoimmune thyroiditis among the three groups (normal, AIT-model and diosgenin groups compared with each other) according to GO term. However, there was a differentially expressed gene in immune research: S100 calcium-binding protein A9 (S100A9). GO enrichment analysis showed that the expression of S100A9 in AIT-model group increased by 3.509 times compared with the normal group, while that in diosgenin group dropped by 0.298 times compared with the AIT-model group. RT-PCR were used to verify it.

4.4 KEGG enrichment analysis of differential genes

The level of distribution of differentially expressed genes and all genes in KEGG Level2 in the diosgenin group compared with the AIT-model group are shown in Figure 4. A bubble diagram of the top 20 KEGG pathways (pathway entries with the number of different genes >2 were selected and sorted according to the -log10Pvalue corresponding to each entry from largest to smallest) is shown in Figure 5.

According to the disease correlation of this study, the cAMP signaling pathway was selected from the top 10 of KEGG enrichment analysis (KEGG Id: rno04024. Enrichment score=6.478567553, pval=0.000994793/padj=0.006610834). In the following mechanism experiment, we detected cyclic adenosine 3',5'-monophosphate(cAMP), protein kinase A (PKA), cAMP response element-binding protein (Creb), exchange protein directly activated by cAMP (Epac), and Ras-related small G protein(Rap1) in the cAMP signaling pathway.

5 Real-time quantitative RT-PCR

Compared with the AIT-model group, in the diosgenin-H group the mRNA relative quantitative expression of Epac and Rap1 decreased from 1 to 0.760 and 0.896 with no statistical significance, PKA and Creb increased from 1 to 2.188 and 1.536 ($P<0.05$), and S100A9 decreased from 1 to 0.368 ($P<0.01$). (Table 3)

6 Immunohistochemical analysis

Under a ×400 light microscope, the immunoreactive substances of cAMP, PKA, and Creb in thyroid tissue appeared brown and were located in the follicular stroma of the thyroid, suggesting that the proteins of cAMP, PKA, and Creb were expressed there (Figure 6). Compared with the normal group, the expression of cAMP(from 0.210 to 0.122), PKA(from 0.235 to 0.116) and Creb(from 0.155 to 0.120) IOD/Area in thyroid tissue of the AIT-model group rats was lower($P < 0.01$). Compared with the model group, the expression of cAMP(from 0.122 to 0.170), PKA(from 0.116 to 0.145), and Creb(from 0.120 to 0.140) IOD/Area in the diosgenin-H group increased with $P < 0.05$.(Table 4)

Discussion

In this study, an AIT model was established by treating rats with high iodine water and injecting porcine thyroglobulin with Freund's adjuvant at multiple points. Female Lewis rats were selected as AIT model rats because they are inbred, highly homozygous, and prone to autoimmune diseases with good repeatability[9]. The results showed that the concentrations of serum TgAb and TPOAb in the AIT-model group were significantly higher than those in the normal group ($P < 0.01$), and a large number of follicular cavities in the thyroid tissue of the AIT-model group were destroyed or reduced in size. Furthermore, the colloid content within the follicles was uneven or decreased, and this was accompanied by lymphocyte infiltration. These results suggested that the AIT rat model was successfully established. Compared with the normal group, serum FT3, FT4 and TRAb in the AIT-model group increased significantly ($P < 0.01$), while TSH decreased, meaning that this AIT rat model was biased to a hyperthyroidism model. When comparing the diosgenin treatment groups with the AIT-model group, the diosgenin low-dose and middle-dose group exhibited slightly improved serum T3, T4, FT3, FT4, TSH, and thyroid antibodies TgAb and TPOAb, but this was not statistically significant. The trends of the low-dose and medium-dose data were similar, suggesting that the concentration of low-dose and medium-dose were insufficient to treat AIT. Compared with the low-dose and middle-dose groups, the diosgenin high-dose group showed improved serum levels, and there was a significant difference when compared with the model group. Pathological results also showed that the infiltration of lymphocytes into thyroid follicular interstitial spaces in the high-dose group was lower, and the thyroid structure was less damaged. Therefore, the thyroid tissue of rats in the high-dose group was selected for transcriptome detection to explore the potential molecular mechanism of the protective effect of diosgenin on AIT rats.

It is difficult to carry out genetic experiments on thyroid tissue, because the thyroid tissue of rats or mice is very small and degrades easily; in addition, there is little related literature on the subject. We extracted the thyroid tissues of 5 rats from the normal, AIT-model, and diosgenin high-dose groups, and extracted their RNA; and the quality inspection results were all qualified. After transcriptome detection, the results were verified by RT-PCR, which agreed with the transcriptome measurements. DESeq software was used to analyze the number of DEGs: in the diosgenin group this was 79, with 54 up-regulated and 25 down-regulated compared with the AIT-model group; these results indicated that diosgenin affected many genes with widely different functions to relieve AIT. GO enrichment analysis showed that the expression

of S100A9 in AIT-model group increased by 3.509 times compared with the normal group, while that in diosgenin group dropped by 0.298 times compared with the AIT-model group. S100A9 is a member of S100 protein family, which is involved in inflammatory reaction[10]. S100A9 level in AIT patients was significantly higher than that in healthy control group[11]. Compared with AIT-model group, S100A9 mRNA decreased by 0.368 times in the diosgenin-H group ($P<0.01$), suggesting that diosgenin may slow down the development of AIT by downregulating the expression of S100A9 gene.

The differential genes were analyzed by KEGG enrichment analysis, and the top 10 terms were as follows: Cardiac muscle contraction, Adrenergic signaling in cardiomyocytes, Oxytocin signaling pathway, Glycosaminoglycan biosynthesis-keratan sulfate, Arrhythmogenic right ventricular cardiomyopathy (ARVC), TGF-beta signaling pathway, cAMP signaling pathway, Insulin secretion, and Hypertrophic cardiomyopathy (HCM). PKA, Creb, Epac, and Rap1 in the cAMP signaling pathway were verified by RT-PCR. The results showed that, compared with the AIT-model group, the relative expression of Epac and Rap1 mRNA in the diosgenin-H group decreased with no statistical significance, suggesting that cAMP might not activate Epac or Rap1 downstream. Meanwhile, the relative expression of PKA and Creb increased ($P<0.05$).

Apoptosis is the main mechanism involved in thyroid cell death[12]. In Graves' disease, there are three thyroid-stimulating hormone receptor(TSHR) antibodies with different functions (stimulating, blocking, and cleavage). The stimulating antibody can induce the survival and proliferation of thyroid cells through cAMP/PKA/Creb, while the cleavage antibody can induce cell death through mitochondrial ROS (mROS), and the generation of cAMP/PKA can also prevent apoptosis by inhibiting mROS[13]. The results of Immunohistochemistry (IHC-P) showed that the IOD/area of cAMP/PKA/Creb in the AIT-model group was lower than that in the normal group, and there was thyroid epithelial cell injury and follicular destruction, which suggested that the low expression of cAMP/PKA/Creb was related to the structural damage to the thyroid tissue. Compared with the AIT-model group, the mRNA and IOD/area of cAMP, PKA, and Creb in the diosgenin group were up-regulated with statistical differences, suggesting that diosgenin may induce the survival and proliferation of thyroid cells through cAMP/PKA/Creb and prevent apoptosis in thyroid cells to some degree.

Previous studies have shown that diosgenin can inhibit the proliferation of thyroid cells by inhibiting the expression of IGF-1, NF-κB, cyclin D1, and PCNA, and alleviating goiter in a Graves' disease murine model [8]. In current study, diosgenin may induce the survival and proliferation of thyroid cells through cAMP/PKA/Creb. So, whether diosgenin can balance the proliferation of thyroid cells by inhibiting IGF-1, NF-κB, cyclin D1, and PCNA and up-regulating cAMP/PKA/Creb is worthy of further study. In addition, in KEGG enrichment analysis, diosgenin can significantly down-regulate the expression of the interleukin (IL)17 signaling pathway. Studies[14] have shown that Th17 cells and Tregs are involved in the pathogenesis and development of AIT. Furthermore, it is known that cellular immune balance of Th17/Tregs plays an important role in AIT[15-16]. So, whether diosgenin down-regulates the expression of the IL-17 signaling pathway and plays a role in Th17/Tregs cellular immune balance is also worthy of

further study. In the current study, we only examined the curative effect *in vivo* along with its corresponding mechanism; an *in vitro* experiment may provide more evidence for the detailed molecular mechanism of AIT.

In summary, the current study suggests that diosgenin can improve the expression of T3, T4, FT3, FT4, and TSH in AIT-model rats, and decrease the concentration of TRAb, TgAb and TPOAb. This mitigation may be related to the activation of the cAMP/PKA/Creb pathway and downregulating the expression of S100A9 gene.

Materials And Methods

Animals

The experiment complied with the Chinese Act on Animal Experimentation, which implements the Directive 2011/588 on the Protection of Animals used for Scientific Purposes. The animal experiments were approved by the Subcommittee of Experimental Animal Ethics of the Academic Committee of Beijing University of Chinese Medicine, no: BUCM-4-2019070303-3003. Working license number of laboratory animal practitioners: 1117052400087. And all experiments were carried out in compliance with the ARRIVE guidelines.

Fifty female SPF(Specific pathogen free) Lewis rats, aged 4 weeks, weighing 80 ± 10 g were purchased from Beijing Vital River Laboratory Animal Technology Co., Ltd, Beijing, China; license no: SCXK (Jing) 2016-0006.

Reagents

Diosgenin (High Performance Liquid Chromatography(HPLC) ≥ 98%, lot: C10J9Q52616. Shanghai Yuanye Bio-Technology Co., Ltd, Shanghai, China.) was dissolved in 0.5% carboxymethyl cellulose sodium salt solution (lot: SL29151601, Coolaber, Beijing, China) and 0.02% dimethyl sulfoxide (lot: 1129E031, Solarbio, Beijing, China) was added to prepare the suspension for subsequent use.

Sodium iodide solution was prepared by dissolving 50 mg of sodium iodide in 100 ml of water to produce a 0,05% solution. It is important to keep this solution away from strong light and to use it immediately following preparation (NaI, CAS no: 7681-82-5, 99% AR, Maya-R).

Preparation of emulsifier: Firstly, a 0.1% porcine thyroglobulin (PTg) solution was prepared with phosphate buffer saline(PBS), and then mixed with complete Freund's adjuvant (CFA) with an equal volume ratio; the mixture was then ground into an emulsion. The final concentration of PTg was 0.05%, i.e. 100 ug PTg/0.2 ml emulsifier. The preparation method of incomplete Freund’s adjuvant (IFA) was the same as for CFA (CFA, lot: SLBW7430, Sigma, St. Louis, MO, USA; IFA, lot: SLBZ0619, Sigma; PTg, lot: 018K7012, Sigma).

AIT induction in rats and drug treatment

Protocol for the AIT animal model [17]

Ten rats were randomly selected as the normal group, and the rest were modeled. From the first week of the experiment, model rats were free to drink 0.064% NaI, while non-model rats were free to drink double distilled water. In the third week, the model rats in each group were immunized for the first time: Thyroid globulin emulsion with CFA was injected into the foot pad, and subcutaneously into the back and neck of rats at multiple points (0.2 ml per injection site). Two series of injections were given with an interval of 2 days during one week. Intensified immunization from the 4th to 8th week: Injections of 0.2 ml were performed into the foot pad and subcutaneously into the back and neck of rats once a week. To verify the success of model building, blood was collected from the orbital vein, and the levels of TPOAb antibody in peripheral serum was detected by Elisa. Three model rats were randomly selected for observation of pathological changes in the thyroid gland.

Fifty rats were randomly divided into a normal group, an AIT-model group, a diosgenin low-dose group, a diosgenin middle-dose group, and a diosgenin high-dose group according to their weight, with 10 rats in each group. After modeling, forty AIT rats were randomly divided into four groups according to their serum TPOAb value. And the drug was administered. Rats in the diosgenin low-dose group (10 mg/kg.d), the diosgenin middle-dose group (20 mg/kg.d), and the diosgenin high-dose group (40 mg/(kg.d) were given corresponding drug suspensions, and rats in the normal group and model group were given the same volume of deionized water 1 ml/100 g.d. The treatments were continuously administered for 8 weeks.

Serum and pathological examination

After treatments were completed, rats were anesthetized with 1% pentobarbital sodium, and blood was taken from the abdominal aorta to obtain serum. T3, T4, FT3, FT4, TSH, TRAb and TgAb were detected at the Beijing Sino-UK Institute of Biological Technology. The expression levels of TPOAb were detected by enzyme-linked immunosorbent assay (TPOAb ELISA Kit, lot: C0336030355, Cusabio, Wuhan, China). Unilateral thyroid lobes were taken and fixed in 4% paraformaldehyde for pathological observation. The contralateral thyroid lobe was immediately placed into liquid nitrogen for transcriptome and PCR detection.

The diosgenin high-dose group was detected by transcriptome(n=5), RT-PCR(n=5) and IHC-P(n=3), excluding diosgenin low-dose and middle-dose group.

Transcriptome

Transcriptome sequencing and analysis were conducted by OE Biotech Co., Ltd., Shanghai, China.

RNA extraction and library preparation

Following the collection of unilateral thyroid lobes from rats, they were quickly placed in liquid nitrogen. Total thyroid lobes RNA was extracted using a mirVana miRNA Isolation Kit (Ambion, Austin, TX, USA)

following the manufacturer's protocol. RNA integrity was evaluated using an Agilent 2100 Bioanalyzer (Agilent Technologies, Santa Clara, CA, USA). Samples with an RNA Integrity Number (RIN) ≥7 were subjected to subsequent analysis. The libraries were constructed using a TruSeq Stranded mRNA LTSample Prep Kit (Illumina, San Diego, CA, USA) according to the manufacturer's instructions. These libraries were then sequenced on an Illumina sequencing platform (Illumina HiSeq X Ten) and 125/150 bp paired-end reads were generated.

Bioinformatic analysis

Quality control and mapping

Raw data (raw reads) were processed using Trimmomatic[18] Reads containing ploy-N and low-quality reads were removed to obtain clean reads. Subsequently the clean reads were mapped to the reference genome using HISAT2[19]

Gene-level quantification, analysis of differentially expressed genes (DEGs), cluster analysis, Gene Ontology (GO), and KEGG enrichment

The fragments per kilobase of transcript per million mapped reads (FPKM)[20] value of each gene was calculated using the Cufflinks package[21], and the read counts of each gene were obtained using HTSeq-count[22]. DEGs were identified using the DESeq[23] R package[24] functions estimateSizeFactors and nbinomTest. A P-value <0.05 and foldChange >2 or foldChange <0.5 were set as thresholds for significantly different expression. Hierarchical cluster analysis of DEGs was performed to explore gene expression patterns. GO enrichment and KEGG[25] pathway enrichment analysis of DEGs were performed, respectively, using R based on hypergeometric distribution.

Transcript-level quantification, analysis of differentially expressed transcript , cluster analysis, GO, and KEGG enrichment

For transcript-level quantification, FPKM and read count values of each transcript (protein_coding) were calculated using Bowtie 2[26] and eXpress[27]. DEGs were identified using the DESeq functions estimateSizeFactors and nbinomTest. A P-value <0.05 and foldChange >2 or foldChange <0.5 were set as the thresholds for significantly different expression. Hierarchical cluster analysis of DEGs was performed to explore transcript expression patterns. GO enrichment and KEGG pathway enrichment analysis of DEGs were performed, respectively, using R based on the hypergeometric distribution.

Real-time quantitative RT-PCR

RNA extraction and real-time quantitative RT-PCR were conducted by OE biotech Co., Ltd., Shanghai, China.

Quantification was performed using a two-step reaction process: reverse transcription (RT) and PCR. Each RT reaction consisted of 0.5 μg RNA, 2 μl of 5×TransScript All-in-One SuperMix for qPCR and 0.5 μl

of gDNA Remover, in a total volume of 10 μl. Reactions were performed in a GeneAmp PCR System 9700 (Applied Biosystems, Foster City, CA, USA) for 15 min at 42 ℃, and subsequently for 5 s at 85 ℃. The 10 μl RT reaction mix was then diluted ×10 in nuclease-free water and held at -20 ℃.

Real-time PCR was performed using a LightCycler 480 Ⅱ Real-time PCR Instrument (Roche, Basel, Switzerland) with a 10 μl PCR reaction mixture that included 1 μl of cDNA, 5 μl of 2×PerfectStartTM Green qPCR SuperMix, 0.2 μl of forward primer, 0.2 μl of reverse primer, and 3.6 μl of nuclease-free water. Reactions were incubated in a 384-well optical plate (Roche) at 94 ℃ for 30 s, followed by 45 cycles at 94 ℃ for 5 s, and then 60 ℃ for 30 s. Each sample was run in triplicate for analysis. At the end of the PCR cycles, a melting curve analysis was performed to validate the specific generation of the expected PCR product. The primer sequences were designed in the laboratory and synthesized by TsingKe Biotech(Beijing, China) based on the mRNA sequences obtained from the National Center for Biotechnology Information(NCBI) database as table 5. The expression levels of mRNAs were normalized to β-actin and were calculated using the $2^{-\Delta\Delta Ct}$ method.

Immunohistochemistry

The main steps of immunohistochemical detection were as follows: dewaxing, hydration, 3% hydrogen peroxide treatment, high temperature antigen repair, goat serum sealing, primary antibody at 4 ℃ overnight, rewarming with PBS washing, dropping secondary antibody, diaminobenzene color rendering, hematoxylin staining, hydrochloric acid and alcohol differentiation, tap water washing, dehydration, and sealing. Photomicrographs were taken under a microscope using an Image-Pro Plus 6.0, Media Cybernetics system to detect absorbance, analyze the integral optical density (IOD/Area) of cAMP (lot: ab76238, abcam, Cambridge, MA, USA), PKA (alpha/beta/gamma, phosphor T197, ab75991, abcam, USA), and Creb (phosphor S133, ab32096, abcam, USA), and to carry out statistical processing.

Statistical analysis

SPSS v20.0 statistical software was used to process the data which were expressed using the mean and standard deviation (x ± sd). The data accords with normal distribution and the variance is homogeneous, which is tested by one-way ANOVA, and LSD method is used for comparison between groups. If the data does not conform to normal distribution or variance is uneven, nonparametric test is used. And appropriate correction for multiple comparisons. A difference was regarded to be statistically significant at $P < 0.05$.

Declarations

Data Availability

Sequencing data for this paper has been deposited in the NCBI Sequence Read Archive (PRJNA674448).

Conflict of Interest

the research was conducted in the absence of any commercial or financial relationships that could be construed as a potential conflict of interest.

Author Contributions

CF.Z. and LL.Q. designed/performed the experiments and wrote the paper; LL.W. and Y.W. contributed to data collection; BJ.S. and FY.Z. helped in data analysis. CF.Z. and LL.Q. contributed equally to this study and share first authorship.

Funding

This paper was supported by Key Laboratory of TCM Health Cultivation of Beijing (grant No.BZ0259) and the Creation and Talent Introduction Base of Prevention and Treatment of Diabetes and Its Complications with Traditional Chinese Medicine (Grant No. B20055). And Subject support from:

1.International science and technology cooperation projects: Study on screening technology and optimization of prescription of traditional Chinese medicine intervention on Hashimoto's thyroiditis(Subject number: 2015DFA30910, Beijing University of Chinese Medicine, China and Harvard University Affiliated McLean Hospital, USA).

2.University-level project of Beijing University of Chinese Medicine: Jiayankangtai development research (Subject number: 1000062520114, Beijing University of Chinese Medicine, China)

Acknowledgments

We thank Liu Wei, Zhao Dan and Qin Shuai for technical assistance. We also thank Charlesworth Author Services for English language assistance and scientific editing.

References

1. CM Buzdugă CF Costea GF Dumitrescu .Cytological, histopathological and immunological aspects of autoimmune thyroiditis: a review. Rom J Morphol Embryol 2017, 58(3):731–738.
2. Yaofu Fan, Shuhang Xu, Huifeng Zhang. Selenium Supplementation for Autoimmune Thyroiditis: A Systematic Review and Meta-Analysis. International Journal of Endocrinology, 2014 , 2014 (1) :904573.
3. Burch H B, Cooper D S. Management of Graves' Disease: A Review[J]. JAMA, 2015, 314(23):2544-2554.
4. McLeod DS, Cooper DS. The incidence and prevalence of thyroid autoimmunity. Endocrine 2012; 42(2):252-265.
5. Janicka K, Jastrzebska I, Petelska AD. The equilibria of Diosgenin–phosphatidylcholine and Diosgenin–cholesterol in monolayers at the air/water Interface. J Membr Biol. 2016;249(4):585-90.

6. Sethi G, Shanmugam MK, Warrier S, Merarchi M, Arfuso F,Kumar AP , et al. Pro-apoptotic and anti-Cancer properties of Diosgenin: a comprehensive and critical review. Nutrients.2018;10(5):645.
7. Bian D, Li Z, Ma H, Mu S, Ma C, Cui B, et al. Effects of diosgenin on cell proliferation induced by IGF-1 in primary human thyrocytes. Arch Pharm Res 2011; 34: 997-1005.
8. Cai H, Wang Z, Zhang HQ, et al. Diosgenin relieves goiter via the inhibition of thyrocyte proliferation in a mouse model of Graves' disease. Acta Pharmacol Sin. 2014;35(1):65-73. doi:10.1038/aps.2013.133
9. Cui SL, Yu J, Shoujun L. Iodine intake increases ip-10 expression in the serum and thyroids of rats with experimental autoimmune thyroiditis. Int J Endocrinol 2014;2014: 581069.
10. Schiopu A, Cotoi OS. S100A8 and S100A9: DAMPs at the crossroads between innate immunity, traditional risk factors, and cardiovascular disease. Mediators Inflamm 2013;2013:828354.
11. Korkmaz H, Tabur S, Savaş E, et al. Evaluation of Serum S100A8/S100A9 Levels in Patients with Autoimmune Thyroid Diseases. Balkan Med J. 2016;33(5):547-551.
12. Morshed SA, Ma R, Latif R, Davies TF. How one TSH receptor antibody induces thyrocyte proliferation while another induces apoptosis. J Autoimmun. 2013; 47:17-24.
13. Morshed SA, Davies TF. Graves' Disease Mechanisms: The Role of Stimulating, Blocking, and Cleavage Region TSH Receptor Antibodies. Horm Metab Res. 2015;47(10):727-734.
14. Li C, Yuan J, Zhu YF, et al. Imbalance of Th17/T reg in Different Subtypes of Autoimmune Thyroid Diseases. Cell Physiol Biochem 2016; 40(1-2): 245-252.
15. Li D, Cai W, Gu R, et al. Th17 cell plays a role in the pathogenesis of Hashimoto's thyroiditis in patients. Clin Immunol 2013; 149(3): 411-420.
16. Liu Y, T ang X, Tian J, et al. Th17/T reg cells imbalance and GITRL profile in patients with Hashimoto's thyroiditis. Int J Mol Sci 2014; 15(12): 21674-21686.
17. Xu XG, Zhang H, Bi XL, Gu J, Shi YL, Hou Q. Xiaoyin recipe for psoriasis induces a Th1/Th2 balance drift toward Th2 in peripheral blood mononuclear cells of experimental autoimmune thyroiditis rats. Chin J Integr Med 2012; 18(2): 137-145.
18. Bolger A M, Lohse M, Usadel B. Trimmomatic: a flexible trimmer for Illumina sequence data[J]. Bioinformatics, 2014, 30(15):2114.
19. KimD, Langmead B and SalzbergSL. HISAT:a fast spliced aligner with low memoryrequirements. Nature Methods, 2015.
20. Adam Roberts, Cole Trapnell, Julie Donaghey, et al. Improving RNA-Seq expression estimates bycorrecting for fragment bias. Genome Biology, 2011.
21. Trapnell C, William B A, Pertea G., et al. Transcript assembly and quantification by RNA-Seq reveals unannotated transcripts and isoform switching during cell differentiation. Nature Biotechnolgy. 2010, 28(5): 511-5.
22. Anders, S., P.T. Pyl, and W. Huber, HTSeq–a Python framework to work with high-throughput sequencing data. Bioinformatics, 2015. 31(2): p. 166-9.

23. Anders, S. and W.Huber, Differential expression of RNA-Seq data at the gene level – the DESeq package. EMBL, 2013.
24. Gupta R, Dewan I, Bharti R, Bhattacharya A. Differential expression analysis for RNA-Seq data. ISRN Bioinform. 2012;2012:817508.
25. Kanehisa M, Araki M, Goto S, etal. KEGG for linking genomes to life and the environment. Nucleic Acids research. 2008, 36:480-484.
26. Langmead, B. and S.L. Salzberg, Fast gapped-read alignment with Bowtie 2. Nature Methods, 2012. 9(4): p. 357-9.
27. Roberts A, et al. Streaming fragment assignment for real-time analysis of sequencing experiments. Nature methods, 2013,10:71-73.

Tables

Table 1 Comparison of serum results of thyroid function(, n=10)

Group	T3(ng/ml)	T4(ng/ml)	FT3(pg/ml)	FT4(pg/ml)	TSH(uIU/ml)
Normal	0.91±0.19	46.75±3.34	1.85±0.15	3.12±0.16	4.37±0.63
AIT-model	1.62±0.32##	86.41±13.23##	3.57±0.35##	5.61±0.75##	2.16±0.26##
Diosgenin-L	1.57±0.28	74.40±11.10	3.05±0.49	4.62±0.49△	2.86±0.36
Diosgenin-M	1.52±0.35	69.54±20.05△	2.86±0.44△	4.38±0.62△△	3.29±0.51△△
Diosgenin-H	1.33±0.20△	65.37±9.30△△	2.66±0.53△△	4.20±0.40△	3.34±0.40△△

Note:#Compared with normal group, P<0.05; ##Compared with the normal group, P<0.01; △Compared with the model group, P<0.05;△△Compared with the model group, P<0.01;

Table 2 Comparison of serum TGAb and TPOAb expression in rats of each group

Group	TGAb (IU/ml)	TPOAb(IU/ml)	TRAb(IU/L)
Normal	24.30±4.98	10.56±0.93	0.94±0.30
AIT-model	147.85±29.40##	168.15±15.10##	24.85±1.25##
Diosgenin-L	96.32±20.15	130.33±15.05	25.27±3.49
Diosgenin-M	87.47±21.92△	125.11±16.30△	21.44±3.07△
Diosgenin-H	80.94±20.44△△	99.94±10.29△△	22.15±3.23

Note:#Compared with normal group, P<0.05; ##Compared with the normal group, P<0.01; △Compared with the model group, P<0.05;△△Compared with the model group, P<0.01;

Table 3 Comparison of PKA, Creb, Epac, Rap1 and S100A9 mRNA expression in thyroid tissue (, n = 5)

gene	AIT-M	Diosgenin	p-value	SD-AIT-M	SD-Diosgenin
PKA	1	2.188	0.039	0.576	1.169
Creb	1	1.536	0.033	0.306	0.381
Epac	1	0.760	0.179	0.329	0.182
Rap1	1	0.896	0.421	0.228	0.078
S100A9	1	0.368	0.001	0.268	0.071

Table 4 cAMP, PKA and Creb IOD/Area expression in thyroid tissue (, n=3)

Group	cAMP	PKA	Creb
Normal	0.210±0.018	0.235±0.032	0.155±0.008
AIT-model	$0.122±0.021^{\#\#}$	$0.116±0.007^{\#\#}$	$0.120±0.016^{\#\#}$
Diosgenin-H	$0.170±0.009^{\#\triangle}$	$0.145±0.014^{\#\triangle}$	$0.140±0.003^{\#\triangle}$

Note:#Compared with normal group, P<0.05; ##Compared with the normal group, P<0.01; △Compared with the model group, P<0.05;△△Compared with the model group, P<0.01;

Table 5: Primer list

Gene	Forward primer (5->3)	Reverse primer (5->3)	length(bp)
S100A9	GCAGCATAAGCACCATCAT	ATTTCTTTGAATTCCGCCTTG	91 bp
PKA	GGACACGAGTAACTTTGACG	AACTCAGTAAACTCCTTGCC	84 bp
Creb	CGCAGGTCCATCAGTTACA	GGATGATGAGAGCCAACGA	105 bp
Epac	CTCCGTGAGGGAAGTGAT	CCGGCAGAATTGACCTTTAC	84 bp
Rap1	CTAAGAGAGCAGATTCTTCGG	GTCTTCCAGGTCGCATTTG	81 bp
β-actin	GCGAGTACAACCTTCTTGC	TATCGTCATCCATGGCGAAC	72 bp

Figures

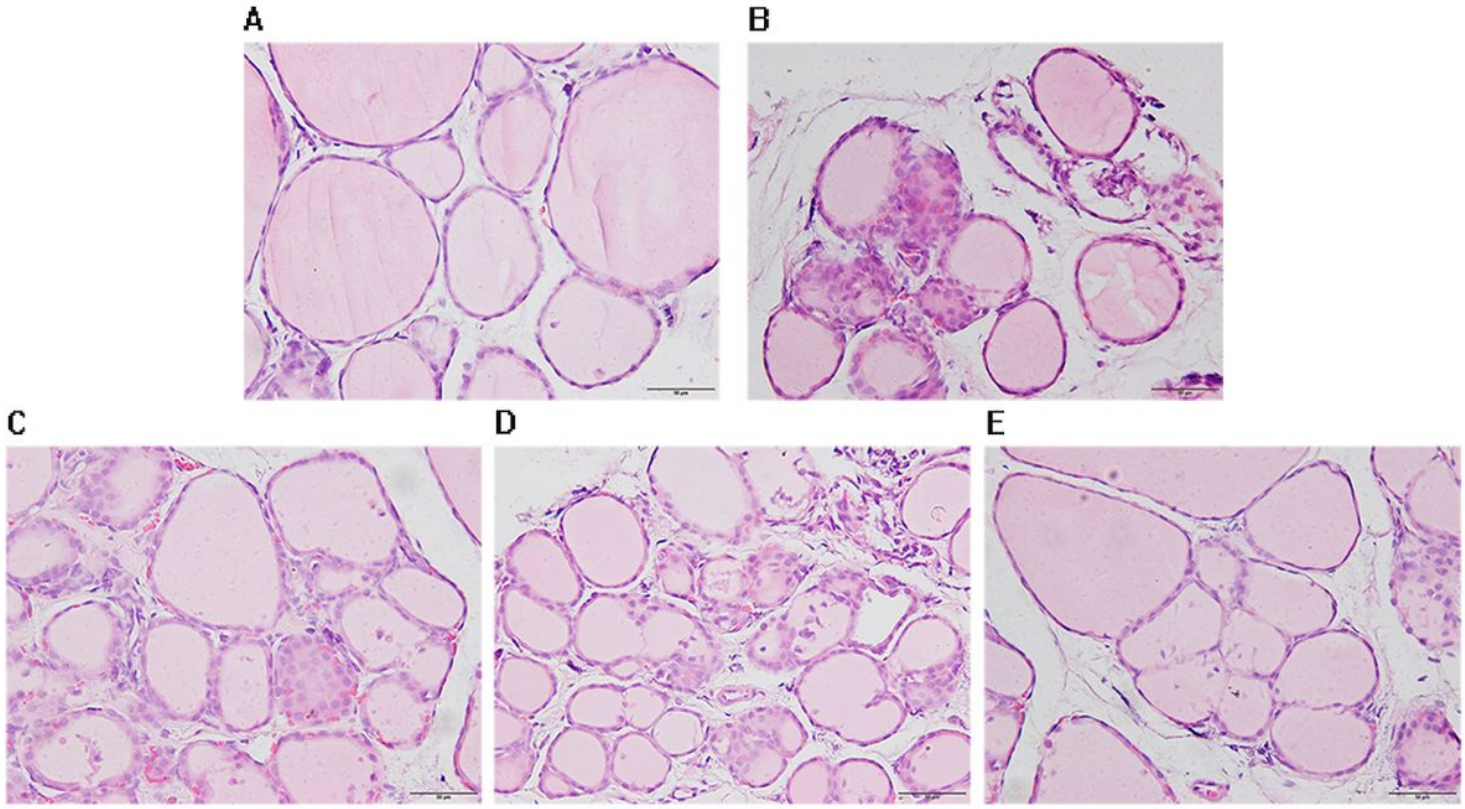

Figure 1

Light microscopic observation results of H&E staining of rat thyroid (×200) A: Normal group, B: AIT-model group, C: Diosgenin-L group, D: Diosgenin-M group, E: Diosgenin-H group

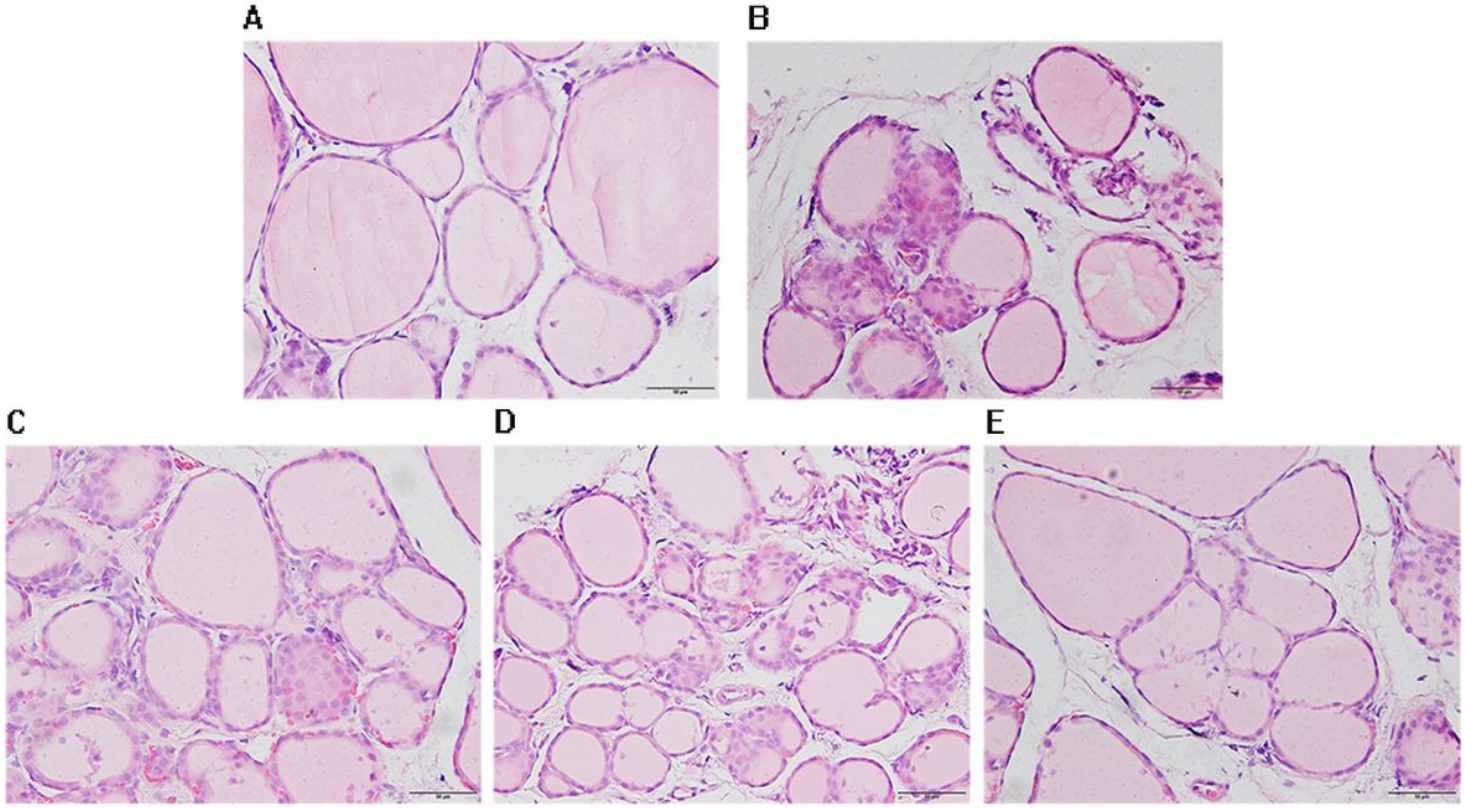

Figure 1

Light microscopic observation results of H&E staining of rat thyroid (×200) A: Normal group, B: AIT-model group, C: Diosgenin-L group, D: Diosgenin-M group, E: Diosgenin-H group

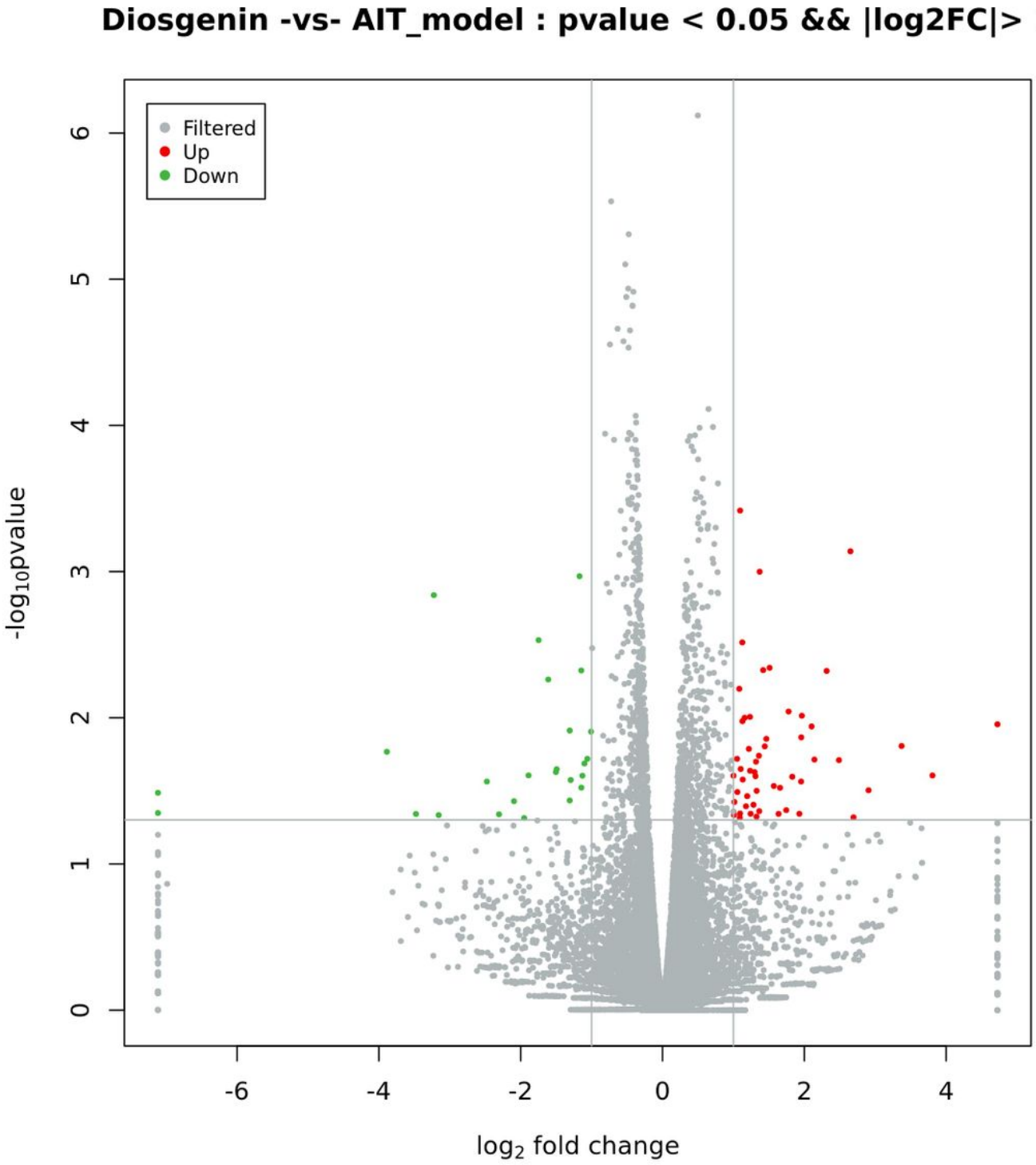

Figure 2

Differential expression volcano map Photo caption: Reflection of the differences caused by comparison in the volcanic map: gray represents those genes with no significant difference, red and green represent the genes with significant differences; the x-axis displays log2FoldChange, and the y-axis displays -log10Pvalue.

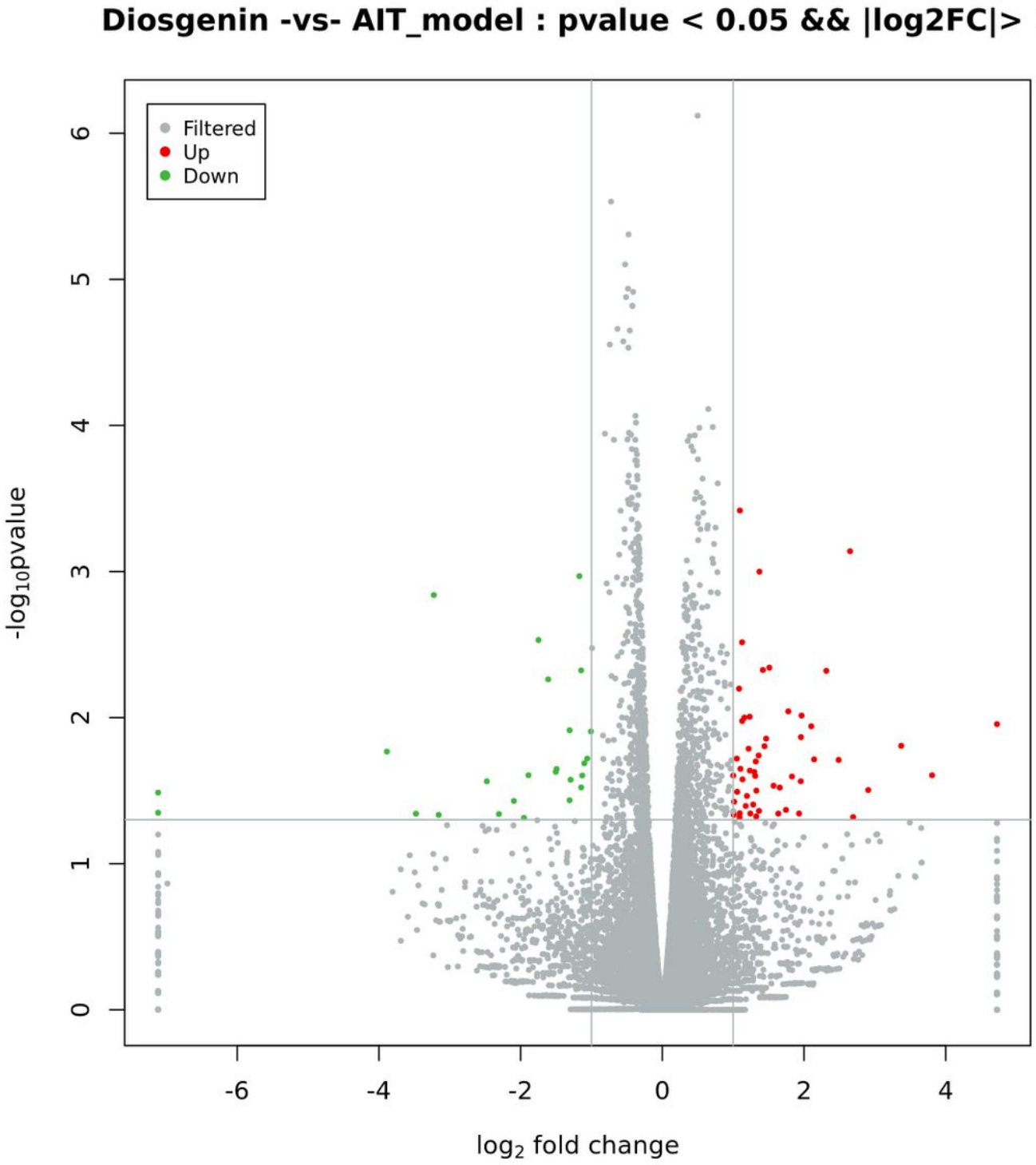

Figure 2

Differential expression volcano map Photo caption: Reflection of the differences caused by comparison in the volcanic map: gray represents those genes with no significant difference, red and green represent the genes with significant differences; the x-axis displays log2FoldChange, and the y-axis displays -log10Pvalue.

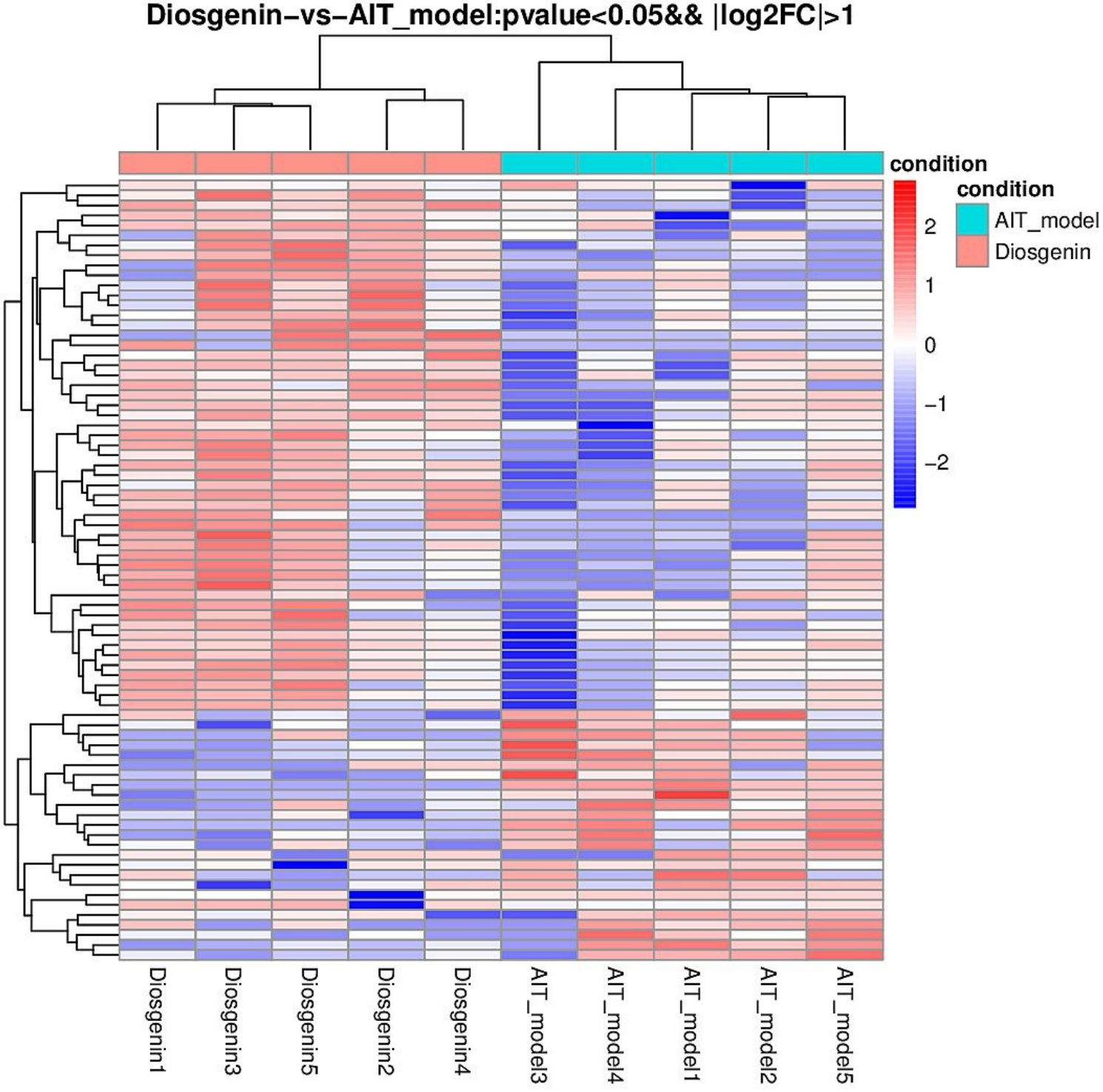

Figure 3

Cluster analysis results of different groups Caption: In the picture, red indicates highly expressed genes, and blue indicates lowly expressed protein-coding genes.

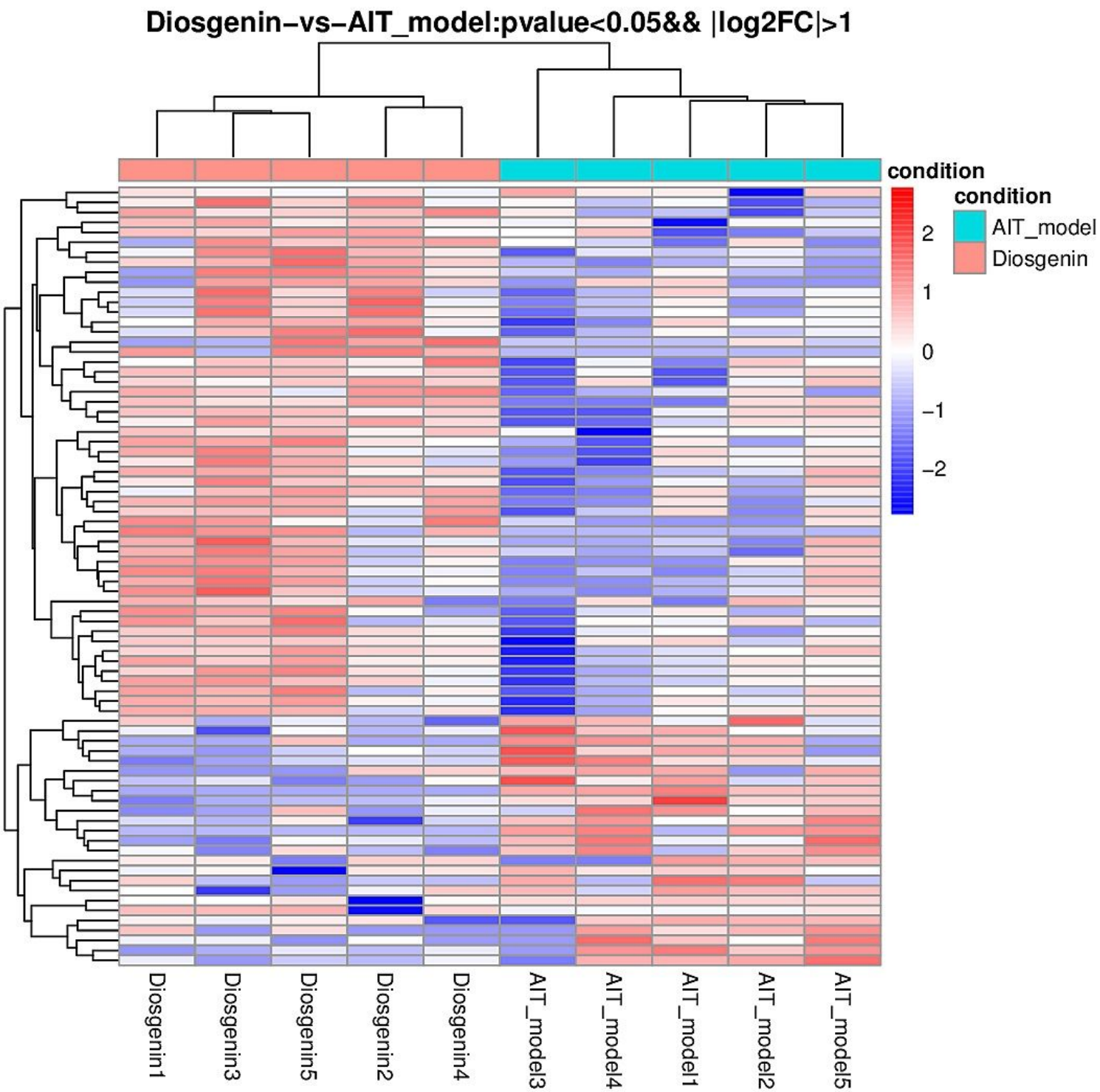

Figure 3

Cluster analysis results of different groups Caption: In the picture, red indicates highly expressed genes, and blue indicates lowly expressed protein-coding genes.

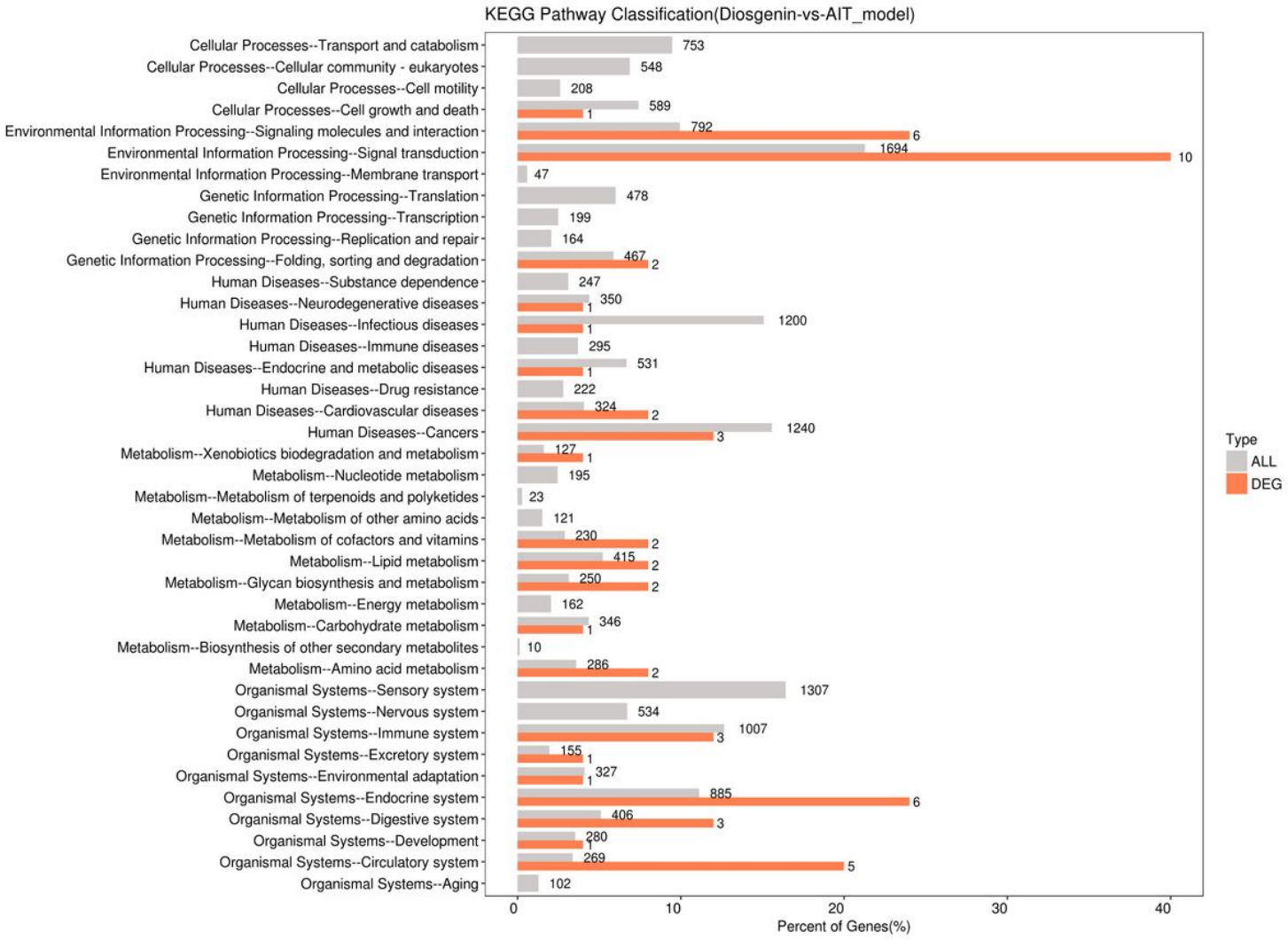

Figure 4

Comparison of differentially expressed genes (DEGs) and horizontal distribution of all genes in KEGG Level2 Photo caption: The horizontal axis is the ratio (%) of the total number of genes annotated to each Level2 metabolic pathway (DEGs) and all genes annotated to KEGG pathway (DEGs), the vertical axis represents the name of the Level2 pathway, and the number on the right side of the column represents the number of DEGs annotated to this Level2 pathway.

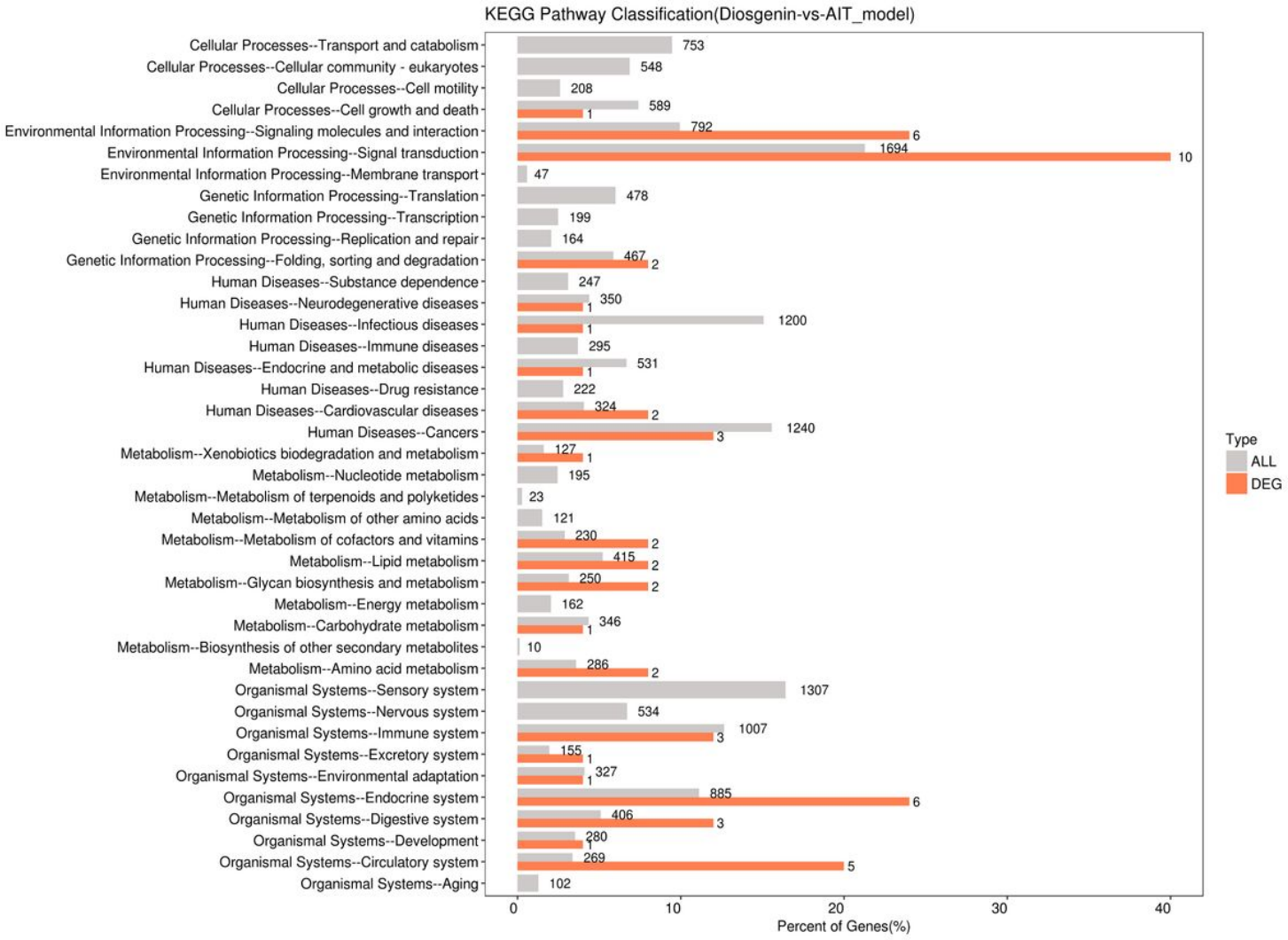

Figure 4

Comparison of differentially expressed genes (DEGs) and horizontal distribution of all genes in KEGG Level2 Photo caption: The horizontal axis is the ratio (%) of the total number of genes annotated to each Level2 metabolic pathway (DEGs) and all genes annotated to KEGG pathway (DEGs), the vertical axis represents the name of the Level2 pathway, and the number on the right side of the column represents the number of DEGs annotated to this Level2 pathway.

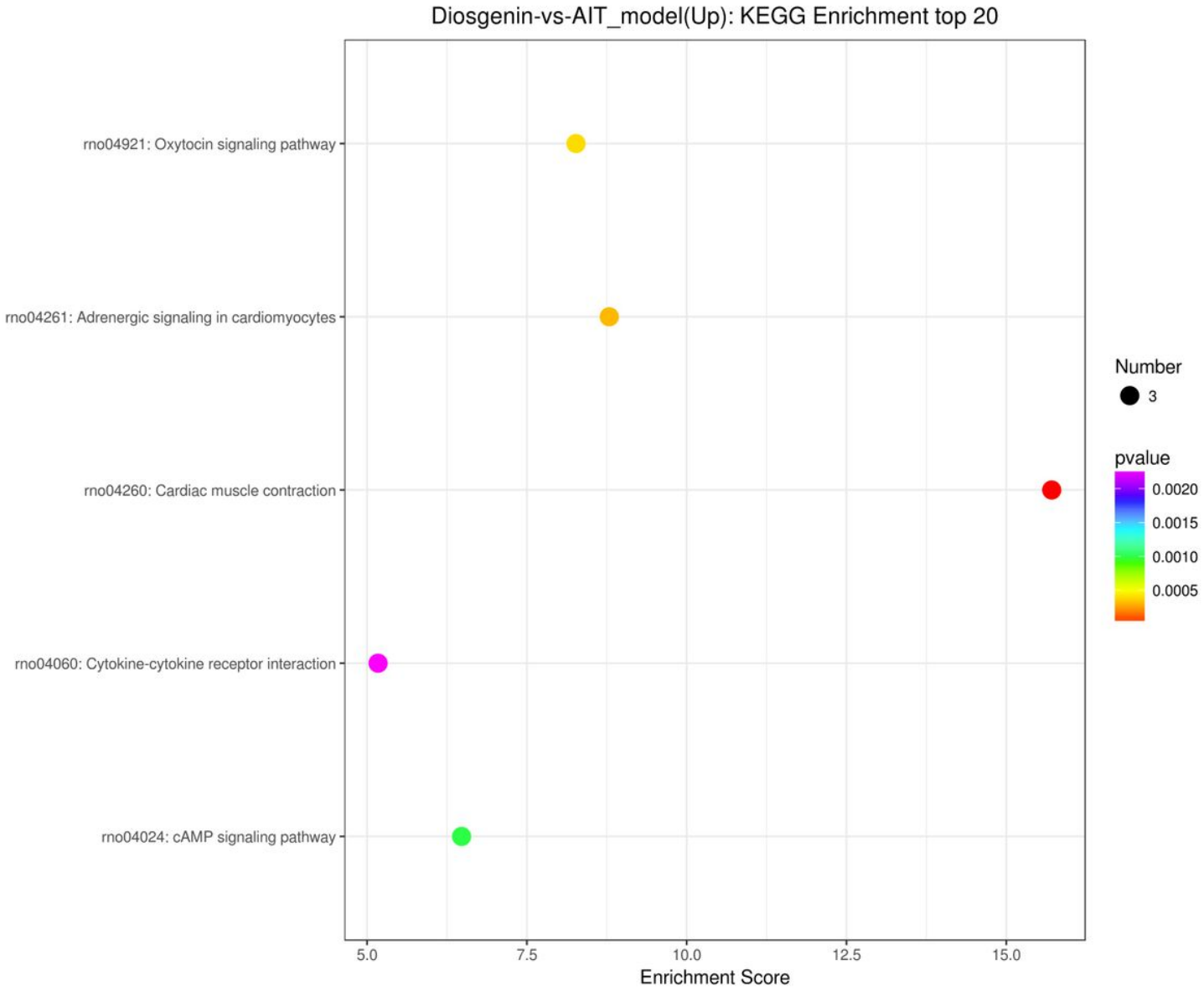

Figure 5

Bubble diagram of top 20 KEGG enrichment analysis pathways Caption: The x-axis displays the enrichment score. The larger the bubble, the greater the number of differential protein-coding genes. The color of the bubble changes from purple-blue-green-red. The smaller the enrichment P-value, the greater the significance.

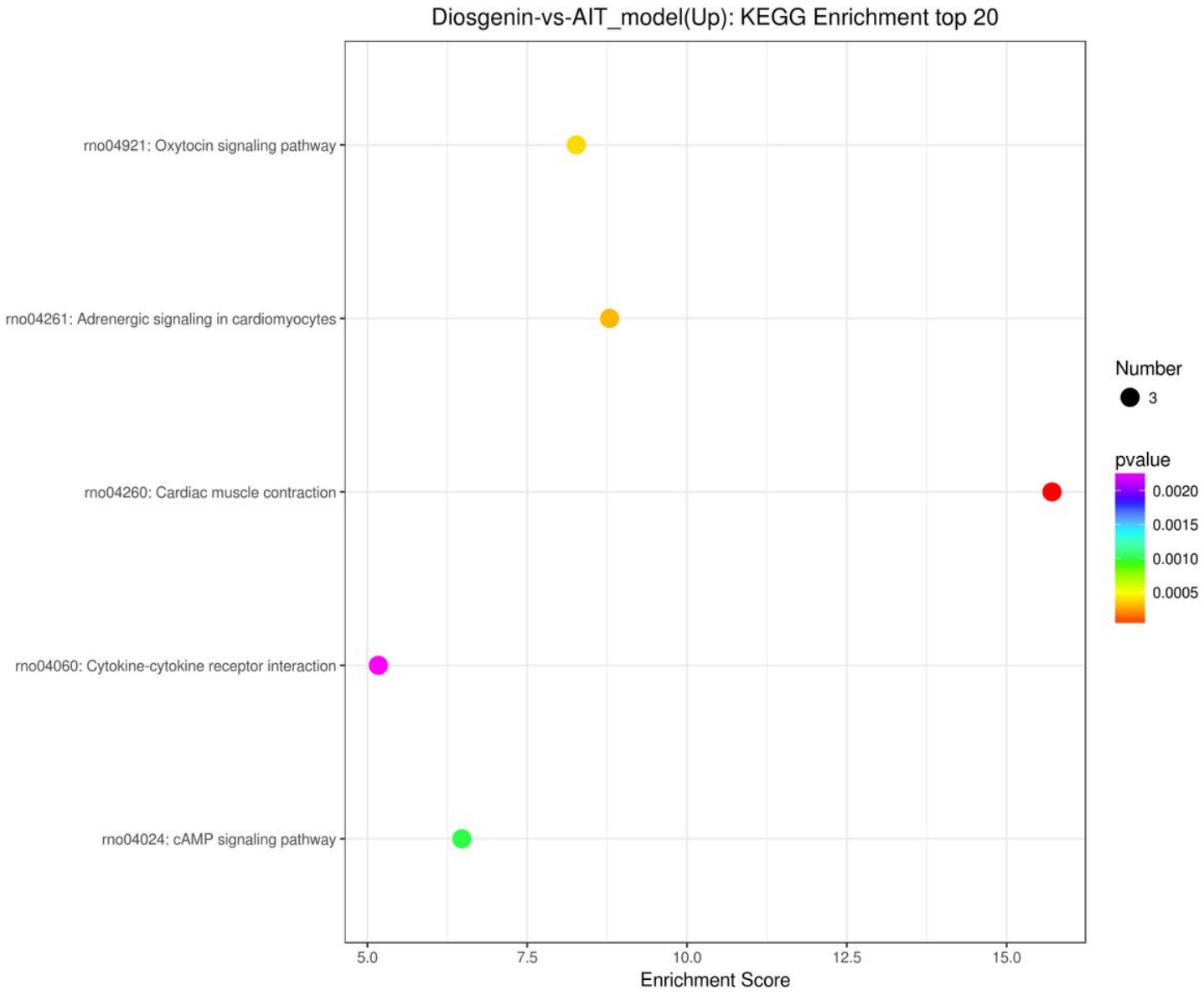

Figure 5

Bubble diagram of top 20 KEGG enrichment analysis pathways Caption: The x-axis displays the enrichment score. The larger the bubble, the greater the number of differential protein-coding genes. The color of the bubble changes from purple-blue-green-red. The smaller the enrichment P-value, the greater the significance.

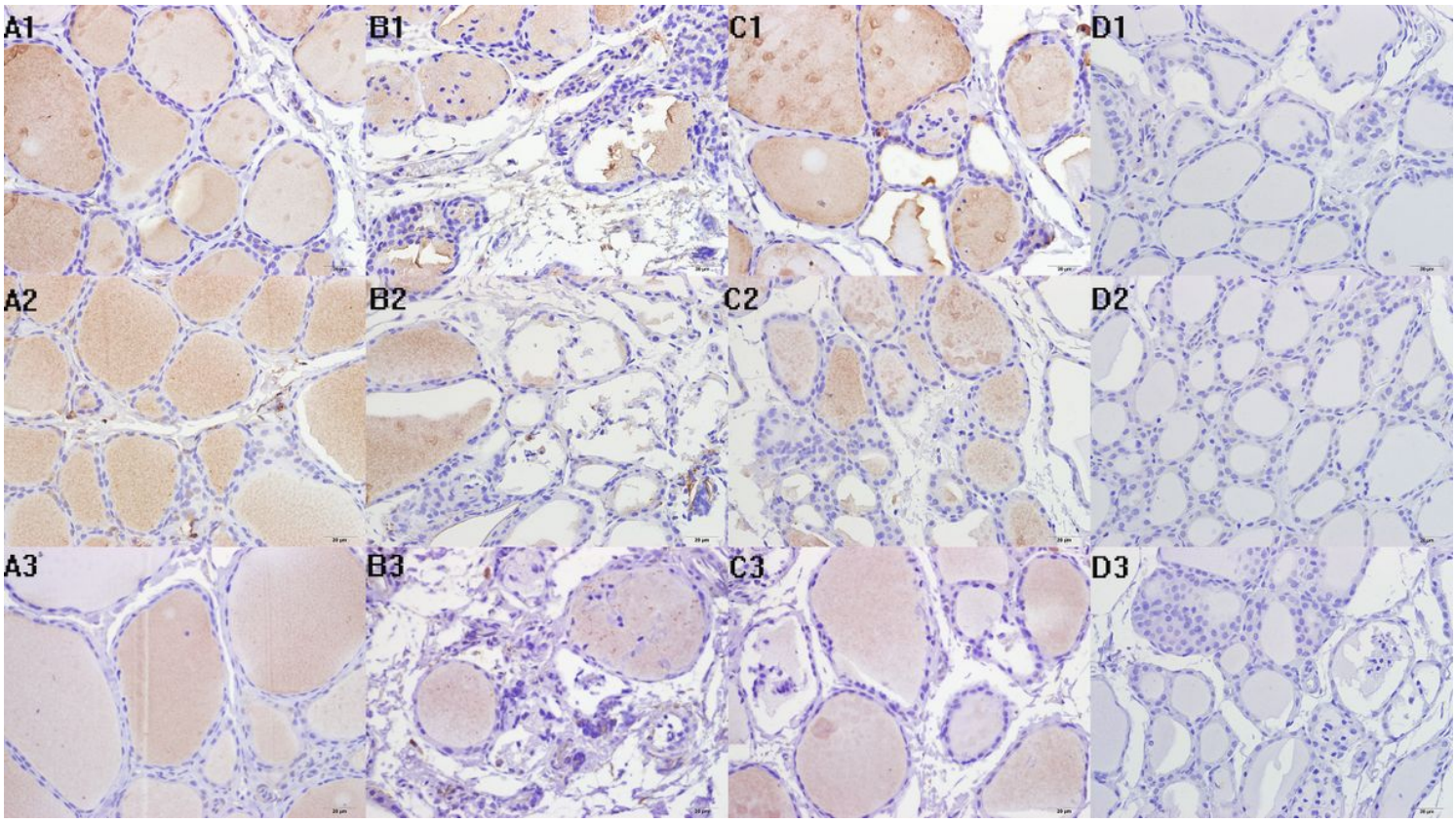

Figure 6

cAMP, PKA, and Creb protein levels in thyroid tissues shown by immunohistochemical staining. A1-D1: cAMP; A2-D2: PKA; A3-D3: Creb. A1, A2, A3: normal control; B1, B2, B3: AIT group; C1, C2, C3: Diosgenin-H; D1, D2, D3: Negative control staining.

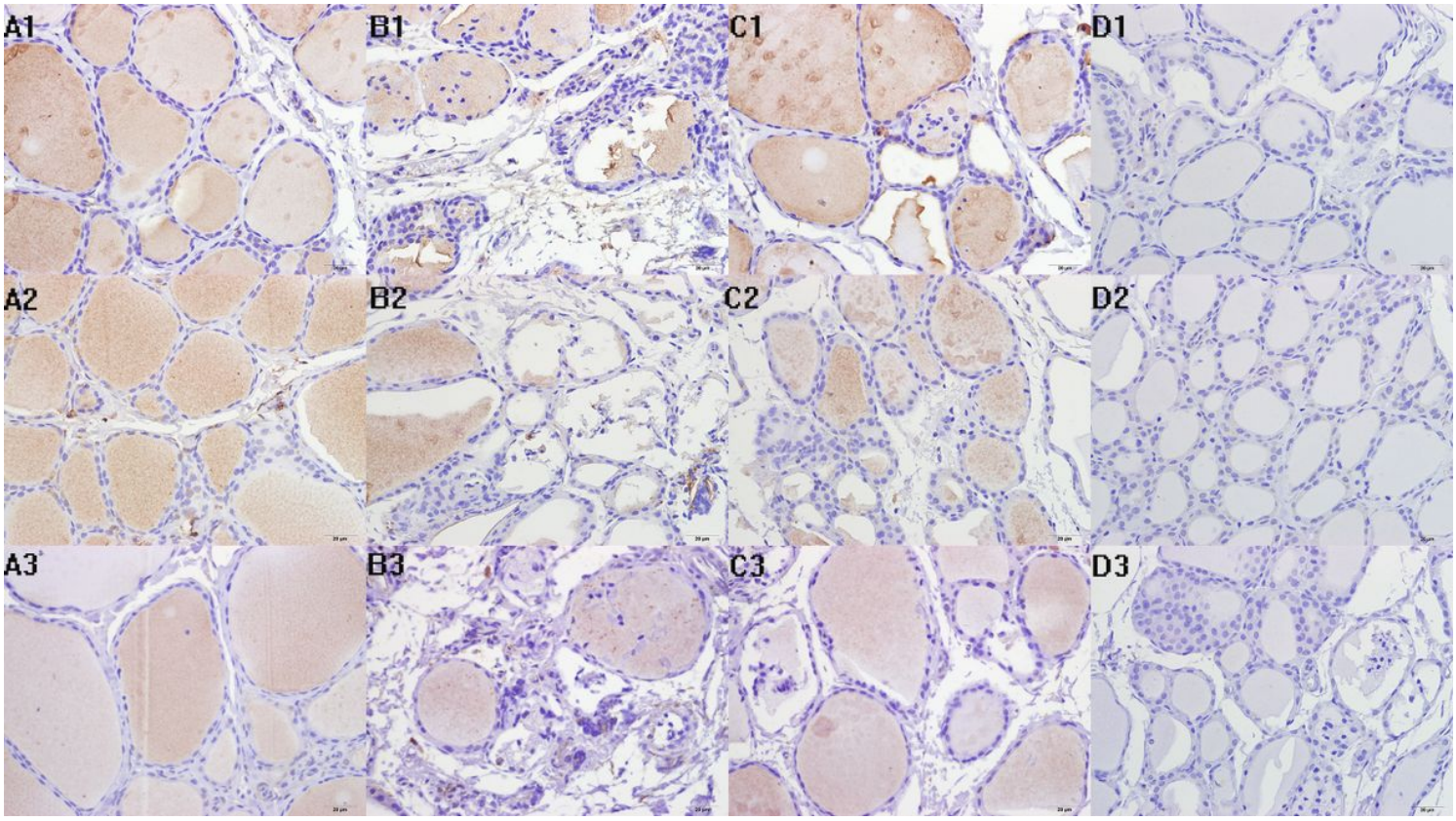

Figure 6

cAMP, PKA, and Creb protein levels in thyroid tissues shown by immunohistochemical staining. A1-D1: cAMP; A2-D2: PKA; A3-D3: Creb. A1, A2, A3: normal control; B1, B2, B3: AIT group; C1, C2, C3: Diosgenin-H; D1, D2, D3: Negative control staining.

Supplementary Files

This is a list of supplementary files associated with this preprint. Click to download.

- SupplementaryMaterialsRNAqualityinspectionresultsofratthyroidtissue.docx
- SupplementaryMaterialsRNAqualityinspectionresultsofratthyroidtissue.docx